Muscle Mitohormesis Promotes Longevity via Systemic Repression of Insulin Signaling

Edward Owusu-Ansah,[1,*] Wei Song,[1] and Norbert Perrimon[1,2,*]
[1]Department of Genetics, Harvard Medical School, Boston, MA 02115, USA
[2]Howard Hughes Medical Institute, 77 Avenue Louis Pasteur, Boston, MA 02115, USA
*Correspondence: ekowuans@genetics.med.harvard.edu (E.O.-A.), perrimon@receptor.med.harvard.edu (N.P.)
http://dx.doi.org/10.1016/j.cell.2013.09.021

SUMMARY

Mitochondrial dysfunction is usually associated with aging. To systematically characterize the compensatory stress signaling cascades triggered in response to muscle mitochondrial perturbation, we analyzed a *Drosophila* model of muscle mitochondrial injury. We find that mild muscle mitochondrial distress preserves mitochondrial function, impedes the age-dependent deterioration of muscle function and architecture, and prolongs lifespan. Strikingly, this effect is mediated by at least two prolongevity compensatory signaling modules: one involving a muscle-restricted redox-dependent induction of genes that regulate the mitochondrial unfolded protein response (UPR^{mt}) and another involving the transcriptional induction of the *Drosophila* ortholog of insulin-like growth factor-binding protein 7, which systemically antagonizes insulin signaling and facilitates mitophagy. Given that several secreted IGF-binding proteins (IGFBPs) exist in mammals, our work raises the possibility that muscle mitochondrial injury in humans may similarly result in the secretion of IGFBPs, with important ramifications for diseases associated with aberrant insulin signaling.

INTRODUCTION

Mitochondria are key organelles that integrate multiple environmental signals. Disruption of mitochondrial function results in the activation of signaling cascades that reflect attempts by the cell to compensate for the effect of perturbed mitochondria, a phenomenon referred to as retrograde or mitochondrial stress signaling (Liu and Butow, 2006). An emerging area of investigation focuses on characterizing the molecular mechanisms of the adaptive cytoprotective responses to low levels of stress, in particular, oxidative stress in the mitochondrion (also referred to as mitohormesis) (Ristow and Zarse, 2010), and how interfering with these responses impacts various metabolic disorders and ultimately aging.

Although severe mitochondrial dysfunction is detrimental, the salutary effects of mild mitochondrial distress have been reported in multiple organisms (Copeland et al., 2009; Dillin et al., 2002; Kirchman et al., 1999; Liu et al., 2005). For example, reducing the expression of some mitochondrial proteins in *C. elegans* and *Drosophila* significantly prolongs lifespan (Copeland et al., 2009; Dillin et al., 2002; Hamilton et al., 2005). In addition, mice mutant for the mitochondrially localized electron transfer redox enzyme p66shc (Migliaccio et al., 1999; Orsini et al., 2004) or the cytochrome *c* oxidase assembly factor (SURF1) (Dell'agnello et al., 2007) have markedly extended lifespans; and importantly, the latter are also resistant to Ca^{2+}-dependent neurodegeneration. Although the exact mechanisms for the beneficial effects of mild mitochondrial distress are unclear, there is growing evidence in the literature to suggest that compensatory stress signaling networks may be a contributing factor. For instance, the increased replicative lifespan associated with mitochondrial perturbation in yeast is abrogated when genes involved in the retrograde response are disrupted (Kirchman et al., 1999), and the prolonged lifespan resulting from electron transport chain (ETC) perturbation in *C. elegans* is reversed by inactivation of some components of the mitochondrial unfolded protein response (UPR^{mt}) (Durieux et al., 2011). Because a complex signaling network is induced in response to mitochondrial perturbation in yeast (Liu and Butow, 2006), it is possible that a broad and diverse set of molecules may be involved in triggering the beneficial effects observed when mitochondrial function is compromised.

We reasoned that by partially disrupting mitochondrial function, it should be possible to examine the stress signaling networks associated with mitochondrial distress in *Drosophila* muscles and the extent to which muscles co-ordinate with other organs to mount an integrated response. We find that muscle ETC perturbation can retard muscle and mitochondrial functional decay, and prolong lifespan, due to compensatory activation of components of the UPR^{mt}, as well as ImpL2 (an ortholog to human IGFBP7) that can bind and inhibit *Drosophila* insulin-like peptides (Alic et al., 2011; Evdokimova et al., 2012; Honegger et al., 2008). Forced expression of UPR^{mt} genes specifically in muscles is sufficient to preserve mitochondrial function and delay age-related locomotory impairment. In addition, muscle mitochondrial distress triggers the upregulation of ImpL2, which represses whole-organism insulin signaling, and augments
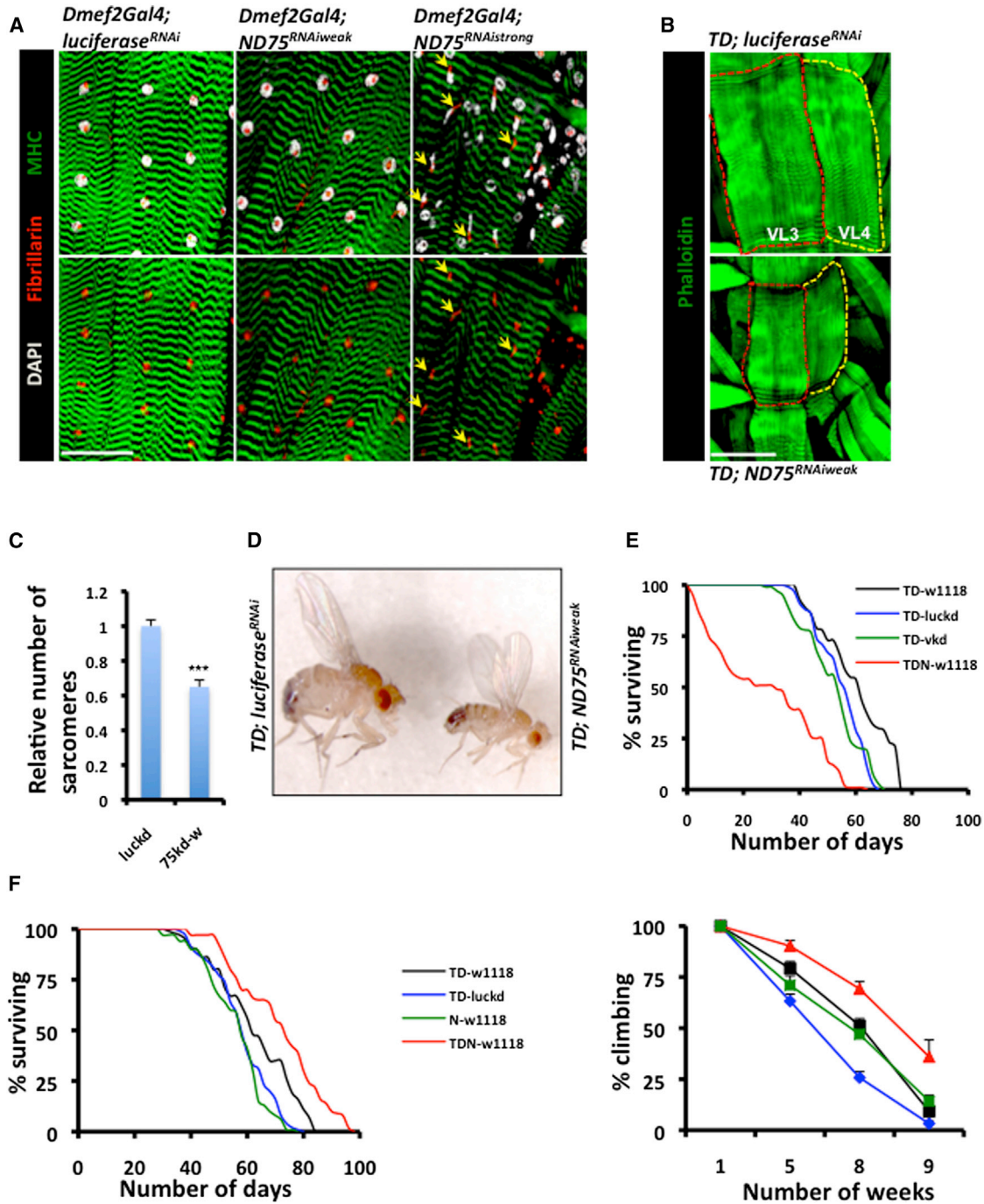
Figure 1. Mitochondrial Perturbation Increases Lifespan and Preserves Locomotory Ability

(A) *Dmef2-Gal4* larval muscles expressing *luciferase*[RNAi] (control), *ND75RNAi-weak* and *ND75*[RNAi-strong] are shown. The sarcomere marker Mhc-GFP, the nucleolar marker Fibrillarin, and the nuclear marker DAPI are shown in green, red, and gray, respectively. Note the nuclear disintegration (yellow arrows) of muscles expressing *ND75*[RNAi-strong]. Scale bar, 75 μm.

(B) Ventral longitudinal 3 and 4 muscle fibers (i.e., VL3 and VL4) expressing *ND75RNAi-weak* (lower) are smaller than aged-matched fibers expressing *luciferase*[RNAi] (top). Scale bar, 75 μm.

(C) Relative number of sarcomeres in VL3 and VL4 muscle fibers of the larval genotypes described in (B) is shown. luckd and 75kd-w refer to *TD; luciferase*[RNAi] and *TD; ND75RNAi-weak* respectively. Error bars denote mean ± SEM (n = 12 muscle fibers). ***p < 0.001.

(D) One hundred and twenty hours of *ND75RNAi-weak* expression in larval muscles result in smaller adult flies (right) relative to controls with larval expression of *luciferase*[RNAi] (left).

(legend continued on next page)

mitophagy by enhancing lysosome biogenesis. Thus, the autonomous induction of the UPR^{mt}, coupled with nonautonomous repression of insulin signaling in response to mild muscle mitochondrial injury, promotes longevity and delays age-dependent muscle functional decline.

RESULTS

Mild Mitochondrial Perturbation in the Larval Musculature Increases Lifespan and Preserves Muscle Function

To examine whether ETC disruption in *Drosophila* muscles can be beneficial, we knocked down the expression of NDUFS1/ND75, a component of complex I. Two different transgenic RNAi lines targeting ND75 were crossed to the Dmef2-Gal4 driver (*Dmef2 >*) to allow muscle-specific knockdown (see Extended Experimental Procedures; Figure S1A available online). One of the lines (i.e., ND75$^{RNAi-strong}$) produced *Dmef2 > UAS-ND75^{RNAi}* animals, which became developmentally arrested around 1.5–2 days after egg deposition (AED) with severe myonuclear disintegration (Figure 1A), whereas the other line (i.e., ND75$^{RNAi-weak}$) gave a weaker phenotype, with larvae arresting after approximately 10 days AED (Figures 1A and S1). Although the latter exhibited smaller muscles, overall muscle integrity was maintained (Figures S1B, S1C, and S2). Interestingly, the delayed muscle growth was associated with the induction of stress response factors such as *4e-bp* and superoxide dismutase 2 (*sod2*) (Figures S1B–S1D). We note that, whereas compensatory stress response factors were induced in larval muscles, they experienced an extended developmental delay and failed to develop into adults (Figure S1E). Thus, to examine whether temporary mitochondrial distress (rather than permanent stress) would allow the larvae to recover to adulthood, we used *tub-Gal80^{ts}; Dmef2-Gal4* (hereafter referred to as TD) to control *ND75$^{RNAi-weak}$* expression (referred to as TDN) because the temperature sensitivity of the Gal80 inactivates Gal4 at 18°C but not at 29°C (McGuire et al., 2004). Larvae were collected at 27°C and shifted to 29°C for different time intervals (Figure S1F). At the end of 120 hr at 29°C (Gal4 fully active), muscle fibers were smaller, and sarcomere assembly was severely impaired in muscles with perturbed mitochondria (Figures 1B and 1C). However, when returned to 18°C (to reduce the extent of mitochondrial distress), they recovered to adults, albeit with reduced adult size and lifespan (Figures 1D and 1E; Table S1). When maintained at 29°C for a shorter duration (24 hr) and then returned to 18°C, the adults that emerged had a markedly increased lifespan relative to controls and maintained their climbing ability longer than age-matched wild-type flies (Figure 1F; Table S1). Importantly, the additional expression of *Gal80* specifically in the muscles (to impair muscle-restricted expression of the RNAi) suppressed the growth inhibition evident in TDN flies after shifting to 29°C, indicating that the phenotypes associated with the transgenic RNAi line are due to muscle-specific expression (Figure S1G). Taken together, these results suggest that, whereas severe and/or persistent mitochondrial injury in muscles is detrimental, mild mitochondrial perturbation has hormetic effects because it delays age-related locomotory impairment and increases lifespan.

Antioxidant Expression Suppresses the Increased Lifespan and Preserved Locomotory Activity Associated with Mild Muscle Mitochondrial Distress

We further observed that TDN muscles had elevated ROS levels relative to controls (Figures 2A and 2B). Depending on the context, elevated ROS levels can be beneficial or cytocidal (Peternelj and Coombes, 2011; Powers et al., 2010). To examine the functional significance of the elevated ROS in this context, we expressed antioxidant enzymes (i.e., enzymes that scavenge ROS) in muscles with ND75 function impaired and examined the effect on longevity and climbing ability. Interestingly, forced expression of catalase (which reduces hydrogen peroxide to water) abolished the enhanced locomotory ability and lifespan of these flies (Figure 2C; Table S2). Because catalase overexpression in the mitochondrial mutant suppresses the lifespan beyond that seen in the wild-type strain, it appears that scavenging ROS uncovers the deleterious effect of complex I perturbation. Similar results were obtained with glutathione peroxidase I (GTPx-1), which also reduces hydrogen peroxide to water (Lubos et al., 2011; Missirlis et al., 2003) (Figure 2D; Table S2). These results indicate that at least one of the signaling axes that conferred tolerance to mitochondrial distress in this context involves a redox-mediated pathway.

Synthetic Lethal Screen to Identify Genes Required for Conferring Tolerance to Muscle Mitochondrial Injury

We designed a synthetic lethal screen to identify RNAi lines that (whereas viable when crossed to TD) produce a lethal phenotype in combination with TDN (see Extended Experimental Procedures; schematic in Figure S3). Significantly, RNAi lines targeting well-established cytoprotective factors such as AMP-activated protein kinase (AMPK), and PTEN-induced kinase 1 (PINK1), which is essential for mitochondrial quality control (Clark et al., 2006), satisfied these two criteria (Table S3). We also identified *Hsp60C* as a gene that is preferentially required in muscles with perturbed mitochondrial function (Table S3).

(E) Lifespan analysis of the adult flies described in (D) is presented. Lifespan curves are for flies that emerged from larvae expressing *ND75RNAi-weak* (red), *vermillion^{RNAi}* (green), and *luciferase^{RNAi}* (blue) in their muscles. The black curve represents flies from a cross between the *TD* driver (see text) and wild-type (i.e., *w1118*) flies.

(F) Lifespan analysis (left) and climbing ability (right) of adult flies that developed from larvae that were collected at 27°C, shifted to 29°C for a day, and returned to 25°C are shown. Color codes are as in (D), except that the green in these panels refers to offspring from a cross between *w1118* and *ND75RNAi-weak*. Error bars in climbing graph indicate mean ± SEM; n = 4 independent cohorts of flies, with the starting number of flies for each genotype in each cohort = 100 and p < 0.05 for TD versus TDN at 5, 8, or 9 weeks. Because *luciferase^{RNAi}* flies had reduced climbing ability as they aged, comparisons are between TDN-w1118 (red) and TD-w1118 (black).

See also Figures S1 and S2. See Table S1 for log rank test, mean, median, and maximum lifespan.
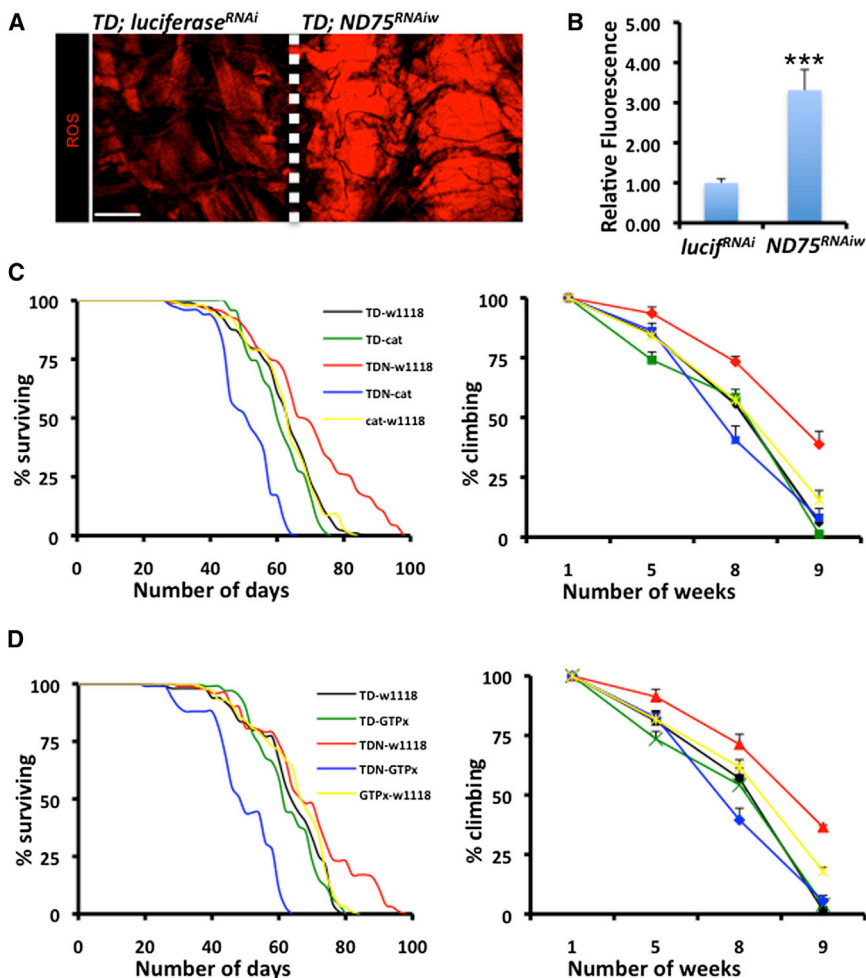
Figure 2. Antioxidant Enzymes Suppress the Enhanced Longevity and Locomotory Behavior Associated with Complex I Perturbation

(A) ROS levels as assessed by DHE are elevated in third-instar larval muscles with ND75 disrupted (right) relative to controls (left). Scale bar, 150 μm.

(B) Mean signal intensities of DHE-stained muscle fibers are shown as described in (A). Error bars denote mean ± SEM (n = 10 samples pooled from two independent experiments). ***p < 0.001.

(C) Lifespan (left) and climbing ability (right) of flies that emerged from larvae collected at 27°C, shifted to 29°C for a day, and returned to 25°C are presented. Genotypes are TDN crossed to *w1118* (red), TDN crossed to catalase (blue), TD crossed to *w1118* (black), TD crossed to catalase (green), and catalase crossed to *w1118* (yellow). Error bars in right panel indicate mean ± SEM (n = 4 independent cohorts with the starting number of flies for each genotype in each cohort = 100; p < 0.01 for TDN-w1118 versus TDN-cat at 8 or 9 weeks). p Value at 5 weeks is 0.129 (not significant).

(D) is similar to (C) but with an alternate antioxidant enzyme GTPx-1, instead of catalase. p < 0.01 for TDN-w1118 versus TDN-GTPx-1 at 8 or 9 weeks. Differences observed at 5 weeks are not statistically significant.

See also Table S2 for additional lifespan data.

Hsp60C is an ortholog of the bacterial GroEL. Orthologs of GroEL in *C. elegans* have been implicated in the UPR^mt, which is a protein quality control mechanism where mitochondrial distress activates the transcription of nuclear-encoded chaperones and proteases to restore protein homeostasis in the mitochondrial matrix (Haynes and Ron, 2010). Other nuclear-encoded mitochondria-localized chaperones are the Hsp70 family member mtHsp70 and the chaperonin Hsp10, an ortholog of bacterial GroES (Haynes and Ron, 2010). There is at least one *Drosophila* ortholog of mtHsp70 (Hsc70-5) and two orthologs of Hsp10 (CG11267 and CG9920). In addition, the protease ClpP resides in the matrix of mitochondria and is involved in the UPR^mt in *C. elegans* (Haynes and Ron, 2010). ClpP functions in concert with ClpX (CG4538 in *Drosophila*). Because Hsp60C disruption is synthetic lethal in mitochondrial mutant flies (Table S3), we hypothesized that the UPR^mt might be an essential adaptive response process that conveys some of the beneficial effects of flies with perturbed mitochondrial function. To test this hypothesis, we performed a synthetic lethal test with the *Drosophila* ortholog of ClpX in the mitochondrial mutant muscles. Similar to Hsp60C, disruption of ClpX in muscles with perturbed mitochondrial function potently compromised viability, while sparing wild-type flies (Table S3).

Adult-Onset Muscle Mitochondrial Perturbation Increases Lifespan and Preserves Mitochondrial and Muscle Function

Because of the developmental delay observed when the mitochondrial mutant larvae are shifted to 29°C, we wondered whether the effects of disrupting the UPR^mt genes were simply developmental, or perhaps degenerative. To resolve these concerns, we analyzed the effect of mitohormesis in adult flies. We compared TD flies (with or without UAS-*ND75RNAi-weak* expression, referred to as experimentals and controls, respectively) raised at 18°C during development but shifted to 27°C as adults to allow disruption of ND75 in muscles during the adult stage (Figure S1F). No overt phenotypic differences or developmental delays were observed when both flies were raised at 18°C (or even up to 25°C) before eclosion. However, when shifted to 27°C, lifespan was significantly increased in flies with ND75 (or other complex I proteins) disrupted in their muscles (Tables S4 and S5). In addition, the elevated temperature at the adult stage accelerated the appearance of mitochondrial-degenerative phenotypes, such that by 6 weeks at 27°C, the mitochondrial DNA copy number of control flight muscles had fallen to about 60% of the value for the experimentals (Figure 3A). The preservation of mitochondrial mass was even more evident in transmission electron microscopy (TEM). Indeed, in control muscles, mitochondrial degeneration was extensive, resulting in large hollow interstitial spaces between remnants of mitochondria and myofibrils. However, mitochondrial morphology in the experimental muscles was largely

preserved, leaving very few voids between the myofibrils and mitochondria (Figures 3B, 3C, S4A, and S4B). In addition, the remaining mitochondria in control muscles had fragmented cristae, in stark contrast to the well-arranged and compact cristae of mitochondria in the experimentals (Figures 3B, 3C, S4A, and S4B). ATP levels were significantly elevated in the experimentals relative to controls (Figure 3D). Finally, citrate synthase (CS) activity, which serves as a surrogate indicator of mitochondrial matrix integrity, was elevated in the mitochondrial mutant muscles relative to control (Figure 3E). Similar results were obtained when dihydrolipoamide dehydrogenase (DLD; another mitochondrial matrix enzyme) activity was assessed (Figure 3F). Finally, by 7 weeks at 27°C, muscle architecture had become severely disordered in control flies, to the point where transected myofibers and severely disrupted sarcomeres were frequently seen; however, none of these features were evident in aged-matched muscles expressing $ND75^{RNAi}$ (Figures 3G–3J).

We next examined various behavioral phenotypes that correlate with disrupted muscle or mitochondrial function (Clark et al., 2006; Greene et al., 2003). Control flies developed the elevated wing phenotype (a property of flies with severe disruption of indirect flight muscle mitochondria; Clark et al., 2006) after 6 weeks at 27°C (Figures 3K and 3L). In contrast, less than 20% of flies expressing $ND75^{RNAi}$ developed this phenotype after 6 weeks (Figures 3K and 3L). In addition, flies expressing $ND75^{RNAi}$ displayed better climbing ability and flight performance when compared to controls (Figure 3L). We note that, whereas RNAi targeting $Hsp60C$ or $ClpX$ suppressed the increased climbing/flight performance and lifespan of TDN flies, it also affected wild-type flies (Figure 3L; Table S5). These results show that basal levels of UPR^{mt} genes are required to sustain normal mitochondrial function as flies age, similar to what has been observed for other critical mitochondrial quality control proteins such as PINK1 and Parkin (Clark et al., 2006; Greene et al., 2003).

Forced Expression of UPR^{mt} Genes Is Sufficient to Preserve Muscle and Mitochondrial Function

We examined whether forced expression of UPR^{mt} genes is sufficient to positively modulate longevity and/or mitochondrial and muscle function. Because there are four paralogs of Hsp60 in *Drosophila* (Hsp60, Hsp60B, Hsp60C, and Hsp60D), we performed synthetic lethal tests to examine if the other three are required in TDN muscles for survival. Although RNAi to Hsp60B or Hsp60D did not affect either TDN or TD, disruption of Hsp60 suppressed the survival of both TDN and TD flies. However, induction of Hsp60 in larval TDN muscles (perhaps as a compensatory response) suggests that it may have a cytoprotective function in addition to its apparent developmental role (Figure S4C). To test this hypothesis and to delineate a cytoprotective role for the UPR^{mt} in muscles, we generated transgenic UAS lines of *Hsp60* and *Hsp60C* and expressed them in muscles using the *Mhc-Gal4* driver at 25°C. No lifespan-promoting effects were observed when the UAS lines were crossed to *w1118* flies (Figure 4A; Table S6). However, although less than 40% of *Mhc-Gal4/w1118* flies survived beyond 80 days, 60%–80% of the flies expressing two independent UAS constructs of either *Hsp60* or *Hsp60C* survived beyond 80 days, suggesting

that they had markedly increased lifespans relative to wild-type controls (Figure 4B; Table S6). In addition, ATP levels and CS and DLD activities were elevated in muscles expressing Hsp60 after 5 weeks at 25°C (Figures 4C–4E), and this was associated with a preservation of locomotory activity of such flies (Figure 4F). These results show that the induction of the UPR^{mt} genes, such as *Hsp60* and *Hsp60C* in muscles, preserves mitochondrial function, promotes longevity, and delays age-dependent muscle functional decline.

Redox Signaling Autonomously Regulates the UPR^{mt}

We explored whether UPR^{mt} genes are induced in TDN muscles as an adaptive compensatory response to mitochondrial injury. Interestingly, within a week of shifting to 27°C, most UPR^{mt} markers were induced in TDN muscles (Figure 5A); an event that was recapitulated when another complex I protein (CG9762), which also results in increased lifespan, was disrupted (Figures 5B and S5; Table S4). Mitochondrial stress signaling typically involves kinases activating specific transcription factors that culminate in the upregulation of genes that compensate for the effect of the dysfunctional mitochondria (Finley and Haigis, 2009). Because overexpression of antioxidant enzymes suppressed the hormetic effects associated with complex I perturbation (Figure 2; Table S2), we hypothesized that at least part of the mechanism that results in increased lifespan and sustained locomotory activity in TDN flies likely involves a redox-sensitive signaling cascade. Accordingly, we searched for redox-sensitive signaling pathways that are concurrently active when UPR^{mt} genes are induced. We observed that the JNK target *puckered* (*puc*) was induced concurrently with UPR^{mt} markers (Figure 5C). Importantly, overexpression of antioxidant enzymes (either GTPx-1 or catalase) abrogated the induction of the JNK target *puc* (Figures 5D and 5E), and several of the UPR^{mt} markers (Figure 5D), indicating that redox signaling regulates UPR^{mt} induction. Additionally, forced expression of the JNK effector transcription factor D-Jun resulted in induction of several of the UPR^{mt} markers (Figure 5F), and disruption of *Jun* (*D-Jun*) abrogated the enhanced lifespan of TDN flies (Table S5). Overexpression of the redox-sensitive NF-κB transcription factor, Relish, also resulted in induction of several of the UPR^{mt} markers (Figure 5G), and we note that although antioxidant expression suppressed the induction of several UPR^{mt} genes, Hsp10 expression was refractory to antioxidant expression (Figure 5D). Thus, there may be additional signaling modules for regulating UPR^{mt} induction independent of the JNK pathway. Nevertheless, these results show that in response to mitochondrial complex I perturbation, a redox-mediated mitochondrial stress signaling network impinging in part on the JNK pathway results in activation of the UPR^{mt}.

ImpL2 Secretion from Muscles with Mitochondrial Distress Triggers Nonautonomous Repression of Insulin Signaling

TDN flies maintained at 29°C for 120 hr and then returned to 18°C had muscles that were considerably smaller than wild-type controls (Figures 1B and 1C). However, wing length was shorter, and the overall size of the flies was also smaller (Figures 1D and 6A), raising the possibility that the growth-inhibiting effect of
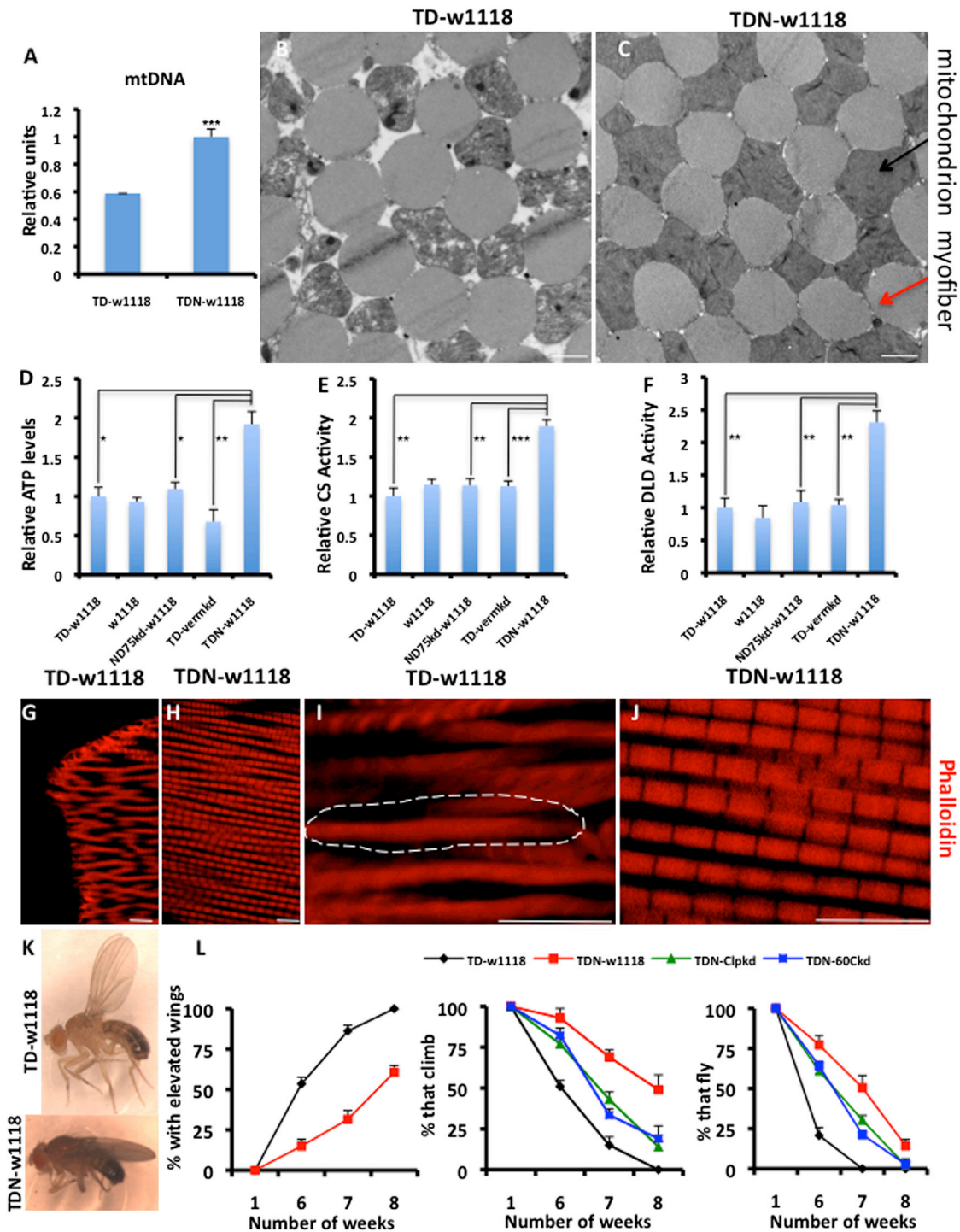
Figure 3. Adult-Onset Muscle Mitochondrial Perturbation Increases Lifespan and Preserves Mitochondrial and Muscle Function

(A) Mitochondrial mass is assessed as relative mitochondrial DNA (mtDNA) levels and is higher in TDN muscles relative to TD (n = 4).

(B and C) TEMs of TD (B) and TDN (C) muscles are shown. Note the large interstitial spaces between remnants of degenerating mitochondria (black arrow) and myofibrils (red arrow) in the TD muscles. Scale bar, 1.0 μm.

(D–F) Relative ATP levels (D), CS activity levels (E), and DLD activity levels (F) are presented. Figure labeling is as follows: (1) *tub-Gal80^{ts};Dmef2-Gal4* crossed to *w1118* labeled as TD-w1118 (negative control); (2) *w1118* (i.e., as wild-type flies); (3) the *ND75RNAi-weak* line crossed to *w1118* labeled as *ND75kd-w1118* (control for insertion site); (4) *tub-Gal80^{ts};Dmef2-Gal4* crossed to a *vermillion^{RNAi}* line labeled as TD-vermkd (RNAi-negative control); and (5) *tub-Gal80^{ts},ND75RNAi-weak;Dmef2-Gal4* crossed to *w1118* labeled as TDN-w1118 (n = 4).
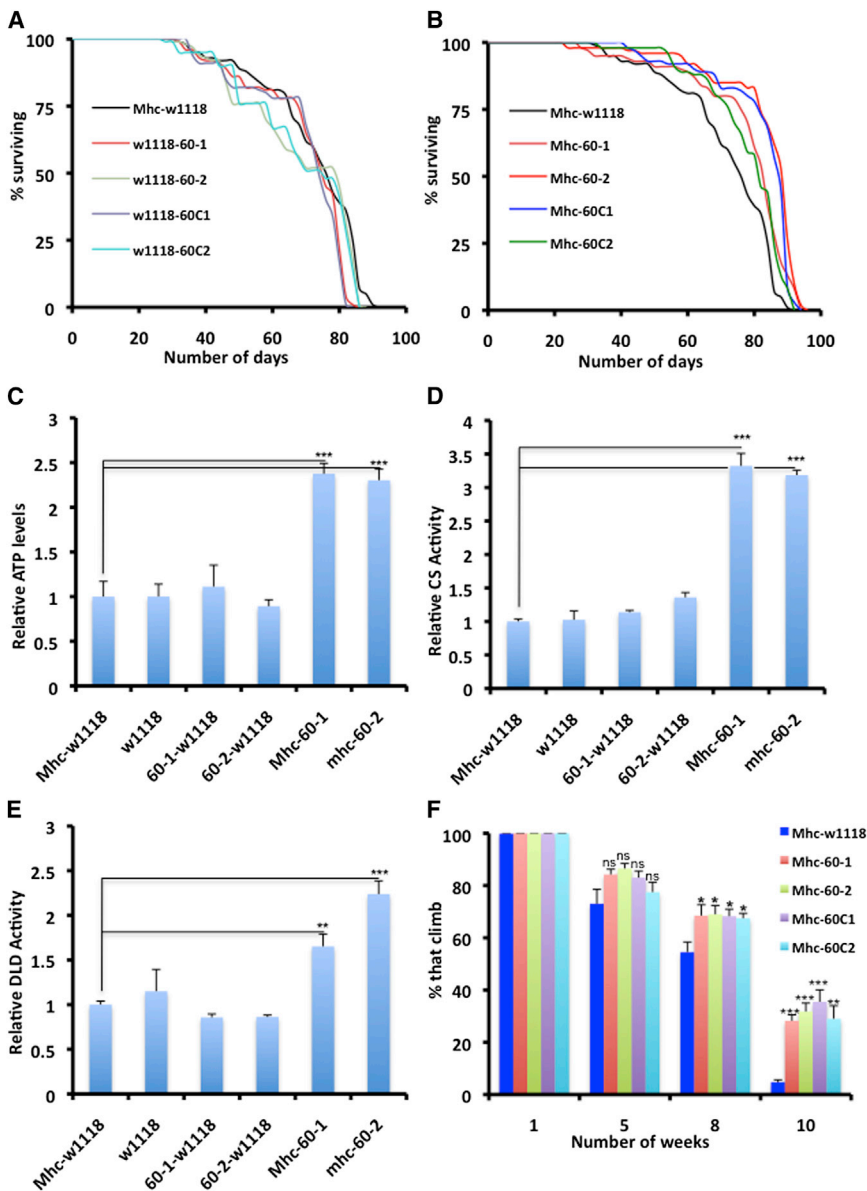
(legend continued on next page)

Figure 4. Forced Expression of UPR^mt Genes Is Sufficient to Preserve Muscle and Mitochondrial Function

(A) Lifespan curves of flies expressing *Hsp60* and *Hsp60C* outcrossed to *w1118* flies, compared to *Mhc-Gal4* flies outcrossed to *w1118* flies, are presented.

(B) Lifespan curves of flies expressing *Hsp60* or *Hsp60C* crossed to *Mhc-Gal4*, compared to *Mhc-Gal4* flies crossed to *w1118* flies, are shown. All transgenes result in an increase in lifespan relative to the background control. Note that the Mhc-w1118 curves are the same in (A) and (B) because the lifespan assays in (A) and (B) were performed concurrently.

(C–E) Relative ATP levels (C), CS activity levels (D), and DLD activity levels (E) of thoraxes from flies with the genotypes listed, after 5 weeks at 25°C, are presented. Figure labeling is as follows: (1) *Mhc-Gal4* crossed to *w1118* labeled as Mhc-w1118 (negative control); (2) *w1118* (i.e., as wild-type flies); (3) *UAS-hsp60* insertion #1 crossed to *w1118* labeled as 60-1-w1118 (control for insertion site #1); (4) *UAS-hsp60* insertion #2 crossed to *w1118* labeled as 60-2-w1118; and (5) *Mhc-Gal4* crossed to *UAS-hsp60* insertion #1 or #2, labeled as Mhc-60-1 and Mhc-60-2, respectively (n = 4). Error bars denote SEM. **$p < 0.01$ and ***$p < 0.001$.

(F) Climbing ability of flies expressing *Hsp60* or *Hsp60C* under the control of the *Mhc-Gal4* driver is illustrated. Data shown are for three independent experiments and are expressed as the mean ± SEM. The starting number of flies for each genotype in each experiment is 100. *$p < 0.05$, **$p < 0.01$, and ***$p < 0.001$. ns, not significant. p Values shown refer to comparisons between the particular genotype and *Mhc-Gal4/w^1118* flies (deep-blue columns). Climbing ability was not preserved when the Hsp60/60C transgenic flies were crossed to *w1118* flies (data not shown).

See also Figure S4C and Table S6.

mitochondrial injury in *Drosophila* muscles may be propagated to other organs/tissues. Interestingly, one of the genes that we identified in our synthetic lethal screen was *ImpL2*. This observation suggested the possibility that ImpL2 may be secreted from flight muscles in the thorax (the muscles with perturbed mitochondrial function) to cause systemic repression of insulin signaling and, thus, contribute to the extended longevity of TDN flies. Strikingly, ImpL2 is induced in flight muscles of the thorax following mitochondrial injury, an event that correlates with the induction of markers of insulin suppression, such as

---

(G–J) Indirect flight muscles of 7-week-old TD (G and I) and TDN (H and J) flies stained with phalloidin (red) to mark the sarcomeres are shown. (I) and (J) are higher magnifications of (G) and (H), respectively (see scale bars). Note the severely disorganized sarcomere structure of TD flight muscles; the broken lines surround an area where the sarcomeres are indistinct, in contrast to the well-arranged sarcomeres of TDN flies. In addition, TD myofibers were frequently found to be transected, as shown in (G). Scale bars, 10 μm.

(K) An example of a TD fly with elevated wings (top) compared to a TDN fly (lower) is shown.

(L) In all panels, TD flies are shown in black, TDN in red, TDN with *ClpX* knockdown in green, and TDN with *Hsp60C* knockdown is shown in blue. Left: most TD flies have elevated wings relative to TDN flies. Middle: climbing ability is preserved in TDN flies as they age, compared to TD flies. Knockdown of *ClpX* or *Hsp60C* suppresses the enhanced climbing ability. Far-right: the flight ability of the flies, which is preserved in TDN flies (n = 4 independent cohorts with the starting number of flies for each genotype in each cohort = 100). $p < 0.001$ for all comparisons between TD and TDN at 6, 7, and 8 weeks.

Error bars denote SEM. *$p < 0.05$, **$p < 0.01$, and ***$p < 0.001$.

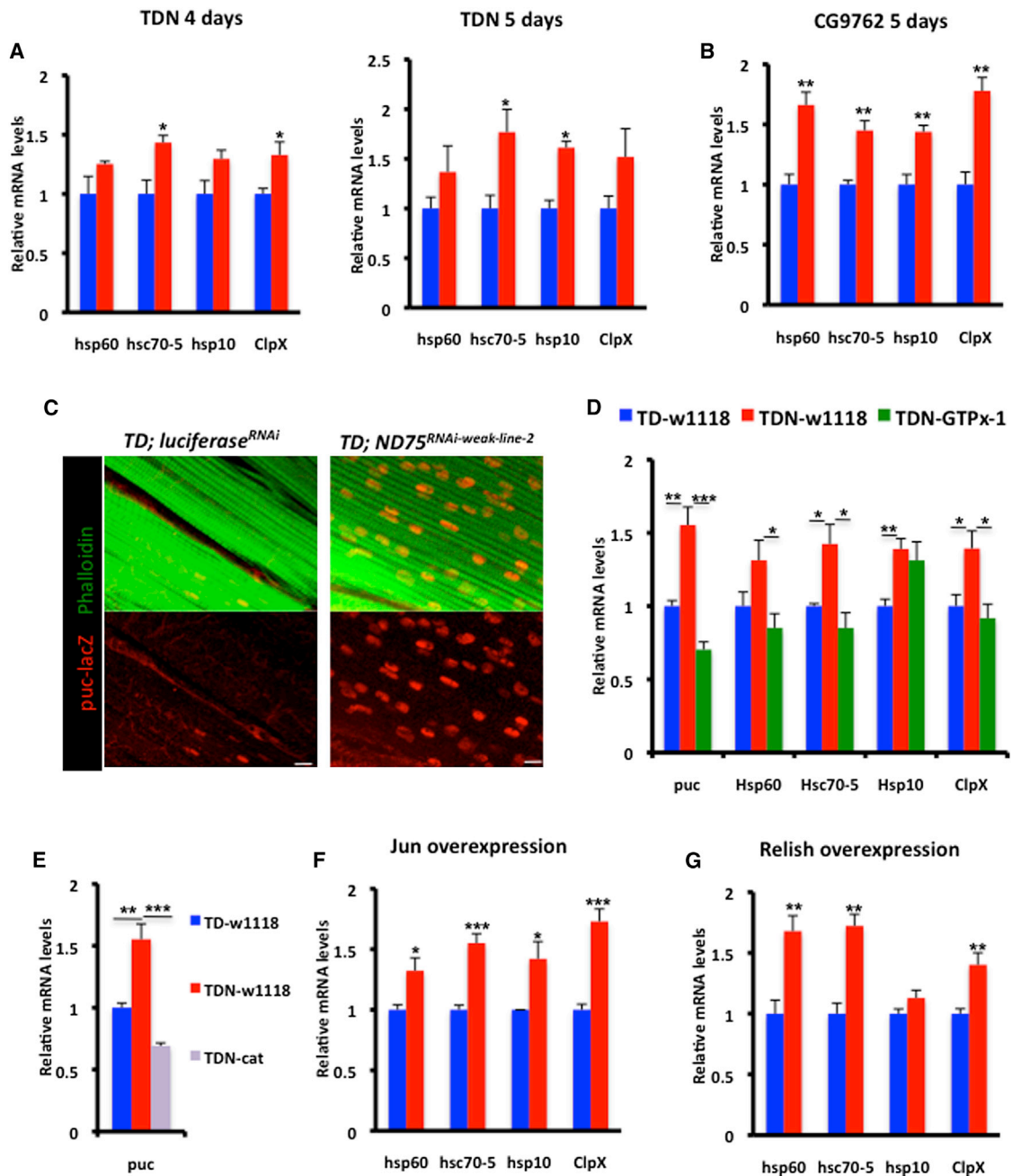See also Figures S3, S4, and S5, and Tables S3, S4, and S5.

Figure 5. Redox Signaling Autonomously Regulates the UPR^mt

(A) Expression of UPR^mt markers in TDN muscles (red) relative to TD muscles (blue) after 4 (left) or 5 (right) days at 27°C is shown.

(B) Expression of UPR^mt markers in CG9762 muscles (red) relative to TD muscles (blue) after 5 days at 27°C is presented.

(C) *puc-lacZ* expression in TD-luciferase^RNAi (left) and TDN (right) muscles is shown. Scale bars, 10 μm.

(D) GTPx-1 expression in TDN muscles suppresses the induction of the JNK target, *puc*, and several of the UPR^mt markers in TDN muscles. TDN is indicated in red, TDN-GTPx-1 in green, and TD control in blue.

(E) The expression of another antioxidant enzyme, catalase, in TDN muscles also suppresses the extent of induction of *puc*.

(F) Expression of UPR^mt markers in muscles expressing the AP-1 transcription factor Jun.

(G) Expression of UPR^mt markers in muscles expressing Relish.

In all qPCR panels, fold induction shown refers to the mean ± SEM (n = 4 independent experiments). *p < 0.05, **p < 0.01, and ***p < 0.001.

See also Tables S4 and S5.

4e-bp and *inr* (Figure 6B) (Karpac et al., 2011). Significantly, *4e-bp* and *inr* were also induced nonautonomously in the abdomen and head (Figure 6B). To further confirm the nonautonomous repression of insulin signaling, we used the tGPH reporter—a fusion protein of GFP and the pleckstrin homology domain of general receptor for phosphoinositides-1 (GRP1), which is recruited to the plasma membrane when cellular levels of phosphatidylinositol-3,4,5-trisphosphate (PIP$_3$) are elevated in response to increased PI3K. In the fat body of TD flies, we observed robust membrane localization of the tGPH reporter; however, in TDN flies, tGPH expression was largely restricted to the nucleus and cytoplasm (Figure 6C). Taken together, we conclude that disruption of complex I in muscles of TDN flies reduces insulin signaling nonautonomously.

Interestingly, forced expression of ImpL2 in flight muscles recapitulated both the autonomous and nonautonomous induction of *4e-bp* and *inr* (Figure 6D); and disruption of ImpL2 function in TDN muscles, via either RNAi or a loss-of-function allele, abrogated the extended longevity of TDN flies, underscoring the importance of systemic repression of insulin activity in response to mitochondrial injury in muscles (Figures 6E, S6A, and S6B; Table S7A). Moreover, larval overexpression of ImpL2 in muscles using the *Dmef2-Gal4* or *Mhc-Gal4* drivers recapitulated the reduced organ size and overall body weight of flies with severely compromised mitochondrial function in their muscles (Figure 6F; also see Figures S6C and S6D). Finally, overexpression of ImpL2 in muscles using either Mhc-Gal4 or TD was sufficient to increase lifespan (Figures 6G and 6H; Tables S7B and S7C).

ImpL2 Expression Increases Lysosome Biogenesis, Possibly to Augment Autophagic Flux in TDN Muscles

Because overexpression of ImpL2 in muscles did not result in UPR^{mt} induction (data not shown), we hypothesized that ImpL2 likely induces an alternate cell maintenance/repair mechanism to confer tolerance to mitochondrial perturbation. Autophagy is an essential catabolic process that sequesters damaged organelles, misfolded proteins, or pathogens in the lysosome for degradation; it generally has a prosurvival function when induced in response to stress (Rubinsztein et al., 2012). Mitophagy is a specific form of autophagy that culls damaged mitochondria into autophagosomes for eventual degradation after fusion with lysosomes. In view of the induction of the UPR^{mt} in TDN muscles, we asked whether mitophagy—an alternate mitochondrial quality control process—is induced in TDN muscles. A transgenic line expressing GFP fused with a mitochondrial-targeting signal (mito-GFP) correctly labels mitochondria in flight muscles (Figure 7A). Because the mitochondrial matrix is enriched with endogenously biotinylated proteins, streptavidin (which binds to biotin) can be used to detect mitochondria, especially in tissues where mitochondria are abundant (Hollinshead et al., 1997). Indeed, in flight muscles, mito-GFP colocalizes with streptavidin (Figure 7A); thus, streptavidin is an appropriate marker for mitochondria in this tissue. Accordingly, to test whether mitophagy is induced in TDN muscles, we examined flight muscles of TDN and TD flies 5 days after shifting to 27°C, for colocalization between autophagosomes (which can be identified as Atg8-GFP punctae) (Rusten et al., 2004) and streptavi-

din. At these early stages of adult life, Atg8-GFP punctae were largely undetectable in TD flight muscles (Figure 7B). However, we detected colocalization between Atg8-GFP and streptavidin in TDN muscles (Figure 7C). To confirm these observations, we examined TEMs of TD and TDN flight muscles at the same time point that the Atg8-GFP punctae were detected. Under normal conditions, mitochondria in flight muscles can be observed in TEM as long parallel stripes (in longitudinal sections) or as a reticular network (in transverse sections) that alternates with myofibrils. In TDN muscles, we reproducibly detected mitochondria that had separated from the reticular network and had become encased in autophagosomes at different stages of formation (i.e., both fully formed and partially formed autophagosomes were observed); however, comparable sequestered structures were not observed in TD muscles (Figures 7D–7G). Because autophagosomes subsequently fuse with lysosomes, we examined whether there were changes in the number of lysosomes. TDN muscles clearly had more lysosomes than TD muscles (Figures 7H–7I); and ImpL2 overexpression potently increased the number of lysosomes, when compared to TD muscles (Figure 7J). Importantly, a loss-of-function allele of ImpL2, which suppresses the extended longevity of TDN flies (Figure S6B), partially suppressed the number of lysosomes formed in TDN muscles (Figure 7K). We note, however, that forced expression of ImpL2 did not significantly alter the number of autophagosomes formed, as assessed by either Atg8-GFP or Hu-LC3-eGFP (data not shown). On the other hand, disruption of Atg6, Atg8A, or Atg12, which are core autophagy genes, abrogated the increased lifespan of TDN flies (Figures 7L and 7M; Table S8). Collectively, these results support a model where mitophagy is upregulated in TDN muscles and that ImpL2 acts primarily to expand the number of lysosomes, possibly to augment autophagic capacity.

DISCUSSION

We have shown that forced expression of genes that regulate the UPR^{mt} is sufficient to retard age-dependent mitochondrial and muscle functional impairment, and overexpression of antioxidant enzymes abolishes the protective effects of muscle mitohormesis due to complex I perturbation. It is noteworthy that exercise physiologists have long acknowledged that interventions to reduce the supposed redox damage in muscles following a bout of physical exercise may actually result in unfavorable alterations to the expression of cytoprotective genes (Peternelj and Coombes, 2011). Our results indicate that a plausible explanation for this effect is that antioxidant treatment dampens the extent of activation of ROS-mediated signaling cascades, culminating in lower levels of mitochondrial repair/maintenance genes required for reestablishing muscle homeostasis following exercise. Our work, coupled with observations in other systems, strengthens the emerging concept that ROS serve as signaling molecules that engage specific signal transduction cascades (Owusu-Ansah and Banerjee, 2009; Owusu-Ansah et al., 2008; Hamanaka and Chandel, 2010; Raimundo et al., 2012; Schulz et al., 2007).

A striking finding of our study is that muscle mitochondrial distress upregulates the insulin-antagonizing peptide (ImpL2),
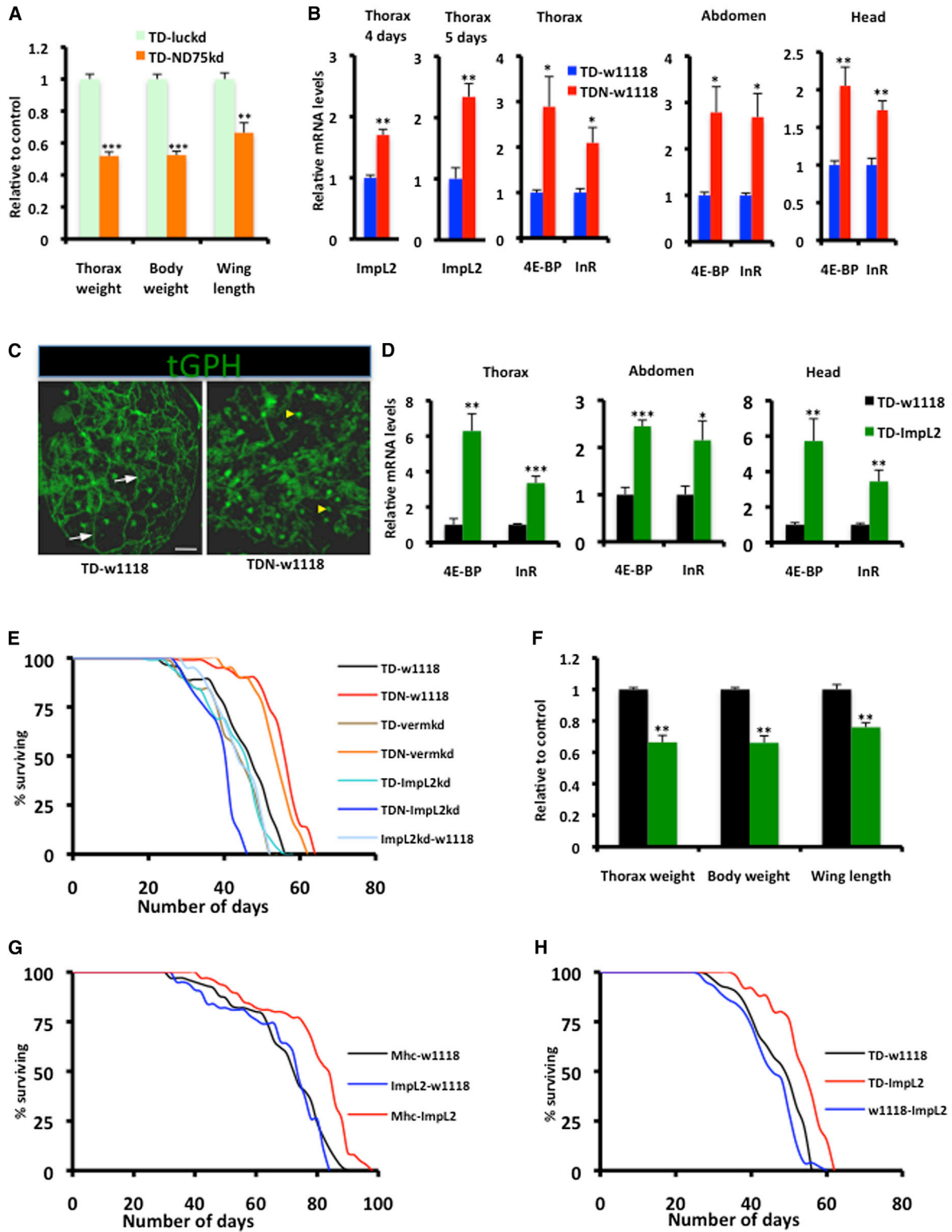
Figure 6. ImpL2 Secretion from Muscles with Mitochondrial Distress Triggers Nonautonomous Repression of Insulin Signaling

(A) Relative thorax weight, overall body weight, and wing length of flies expressing RNAi to ND75 (TD-ND75kd) relative to control flies expressing RNAi to luciferase (TD-luckd) are presented. Larvae were collected at 29°C for 120 hr and then returned to 18°C until adults eclosed. In each instance, n = 4 cohorts, with each cohort consisting of 20 flies.

(legend continued on next page)

which nonautonomously represses insulin signaling. Under adverse environmental conditions, different organs must have the capacity to mount a coordinated adaptive response to the stressor. For instance, the recently discovered exercise-induced Irisin can increase energy expenditure to improve glucose homeostasis (Boström et al., 2012). It is interesting that ImpL2 secretion in response to muscle mitochondrial distress also acts in an adaptive manner by stimulating lysosome biogenesis, possibly to enhance prosurvival autophagy, an event that is critical for survival under stress. Notably, in an analogous situation in the heart, sublethal ischemia is known to trigger the release of cardiomyokines that act in an adaptive manner to preserve myocardial tissue health (Glembotski, 2011).

The idea that mitochondrial respiratory chain deficiency in one tissue can alter events in another tissue has also been observed in *C. elegans*, where RNAi-mediated knockdown of cytochrome *c* oxidase-1 subunit Vb in neurons activates the UPR^{mt} autonomously in neurons and nonautonomously in the gut (Durieux et al., 2011). As a plausible explanation for the nonautonomous effect of mitochondrial respiratory chain deficiency, the authors hypothesized that a specific signal(s) may be secreted in response to mitochondrial dysfunction in one tissue, to subsequently propagate the mitochondrial stress signal to other tissues. Our studies in *Drosophila* show that in addition to the UPR^{mt} other mitochondrial stress responses (in this case, insulin repression) can be transmitted between different organs as well. Accordingly, there may be multiple mechanisms and longevity-promoting signals required for propagating mitochondrial stress responses between organs/tissues.

It has been hypothesized that the various compensatory signaling modules activated in response to mitochondrial dysfunction are not necessarily independent processes but, rather, are a part of a complex mitochondrial regulatory network with multiple axes operating in unison to enhance survival under stress (Andreux et al., 2013). Interestingly, our data support this notion; we find that at least two mitochondrial quality control processes—the UPR^{mt} and mitophagy—are concurrently active in complex I-disrupted muscles. Importantly, whereas forced

expression of UPR^{mt} genes recapitulates many of the phenotypes associated with the preservation of mitochondrial function (Figure 4), lifespan increase was less robust, when compared to the effect of ImpL2 overexpression. Thus, it appears that the UPR^{mt} and ImpL2-dependent pathways regulate different facets of an intricate mitochondrial stress response network: induction of the UPR^{mt} serves primarily to preserve or restore mitochondrial function, whereas ImpL2 induction increases lysosome biogenesis that will enhance the clearance of damaged mitochondria through mitophagy. Interestingly, by selectively culling dysfunctional mitochondria from an otherwise normal pool, mitophagy may augment lifespan by ensuring the propagation of mitochondria with optimum function. The mechanism(s) triggering the longevity-enhancing effect of ImpL2 is likely to extend beyond mitophagy because ImpL2 may help remove misfolded protein aggregates, as has been shown for FOXO/4E-BP signaling (Demontis and Perrimon, 2010). In addition, 4E-BP overexpression is sufficient to increase lifespan and is required for regulating metabolism under stress (Demontis and Perrimon, 2010; Teleman et al., 2005); accordingly, it may play a role in this context as well. Undoubtedly, future studies should help resolve the full breadth of cytoprotective processes that contribute to the lifespan-promoting effect of ImpL2.

In summary, we uncover a mechanism by which mitochondrial perturbation in muscles can cause systemic effects. Given that the human ortholog of ImpL2 (IGFBP7) has recently been shown to bind to the IGF-1 receptor and blocks activation of insulin-like growth factors (Evdokimova et al., 2012), it is enticing to speculate that muscle mitochondrial injury in humans could also lead to upregulation of IGFBP7 (or other IGFBPs) to cause systemic repression of insulin signaling. Such an event will have implications for the known association between mitochondrial dysfunction and diseases associated with aberrant insulin signaling, such as type 2 diabetes. Interestingly, circulating IGFBP7 levels are elevated in patients with type 2 diabetes (Kutsukake et al., 2008); whether this elevation is due partly to muscle mitochondrial dysfunction remains to be tested. Unquestionably, future studies in *Drosophila* and other systems to identify additional signaling molecules elevated in response to mitochondrial

(B) ImpL2 is induced in TDN flight muscles relative to TD flight muscles at 4 (first panel, from left) and 5 (second panel) days after shifting adult flies to 27°C. This correlates with the induction of 4E-BP and InR in flight muscles (thorax) of TDN flies (third panel). In addition, these markers are induced nonautonomously in the abdomen (fourth panel) and head (fifth panel) of TDN muscles.

(C) Localization of tGPH (a PI3K activity reporter) in fat body from TD (left) and TDN (right) flies is shown. Note the extensive membrane recruitment of tGPH (white arrows) in fat body from TD flies. However, in fat bodies from TDN flies, expression of the reporter was largely restricted to the nucleus (yellow arrowheads) and surrounding cytoplasm. Scale bar, 20 μm.

(D) Overexpression of *ImpL2* in the thorax results in the induction of targets of insulin repression in the thorax (left) as well as in the abdomen (middle) and head (far right).

(E) Lifespan curves of flies expressing TDN or TD with various transgenes are shown. The increased lifespan of TDN flies outcrossed to w1118 flies (red, TDN-w1118) or *vermillion^{RNAi}* (orange, TDN-vermkd, which serves as a negative control for RNAi expression) is suppressed when TDN is crossed to *ImpL2^{RNAi}* (blue, TDN-ImpL2kd).
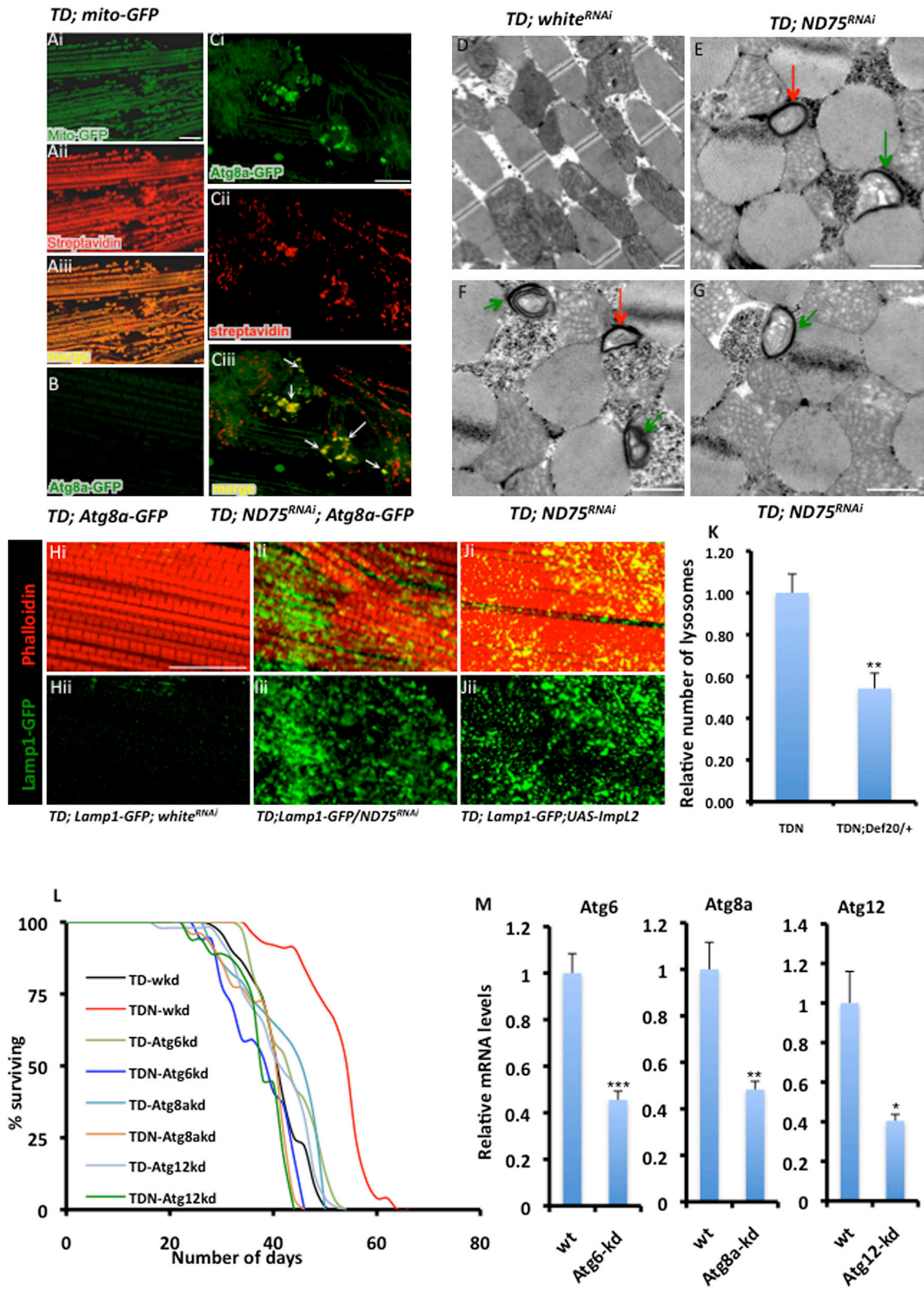
(F) Thorax weight, total body weight, and wing length of flies expressing ImpL2 (TD-ImpL2) relative to control flies (i.e., TD-w1118) are presented. In each instance, n = 4 cohorts, with each cohort consisting of 20 flies. Note the considerably smaller thoraxes, total body weight, and shorter wing length of TD-ImpL2 flies relative to TD-w1118 controls.

(G) Lifespan curves of flies expressing *UAS-ImpL2* outcrossed to *w1118* flies compared to *Mhc-Gal4* flies outcrossed to *w1118* or *UAS-ImpL2* flies are shown. Lifespan was performed at 25°C.

(H) Lifespan curves (performed at 27°C) of flies expressing *UAS-ImpL2* outcrossed to *w1118* flies, compared to TD flies crossed to *w1118* or *UAS-ImpL2* flies are presented.

In all panels, fold change shown refers to the mean ± SEM. *p < 0.05, **p < 0.01, and ***p < 0.001 (n = 4 independent experiments).

See also Figure S6 and Table S7.

TD; mito-GFP

TD; white^RNAi — TD; ND75^RNAi

TD; Atg8a-GFP — TD; ND75^RNAi; Atg8a-GFP — TD; ND75^RNAi — TD; ND75^RNAi

TD; Lamp1-GFP; white^RNAi — TD;Lamp1-GFP/ND75^RNAi — TD; Lamp1-GFP;UAS-ImpL2

(legend on next page)

perturbation are likely to open up therapeutic opportunities for many metabolic diseases.

EXPERIMENTAL PROCEDURES

Drosophila Strains and Genetics
For a list of stocks used, statistical analyses, and detailed experimental conditions, see the Extended Experimental Procedures.

Immunostaining
Larval somatic muscles or adult thoraxes were dissected in PBS, fixed in 4% formaldehyde in PBS for about 30 min (1 hr for thoraxes) at room temperature, and stained following standard procedures.

Electron Microscopy
Electron microscopy was performed essentially as described by Bai et al. (2007).

ROS Staining with DHE
ROS levels were monitored using the superoxide indicator dihydroethidium (DHE), as described by Owusu-Ansah and Banerjee (2009) and Owusu-Ansah et al. (2008).

CS and DLD Activity Assays
CS and DLD activity assays were assessed essentially as described by Rera et al. (2011) and Berger et al. (1996), respectively.

ATP Assay
ATP levels were assessed with the ATP assay kit from Molecular Probes (A22066), following the manufacturer's instructions.

Quantitative Real-Time RT-PCR Analyses of Transcript Levels
RNA was extracted with TRIzol reagent, digested with DNase I, and reverse transcribed using the iScript cDNA Synthesis kit (Bio-Rad), after which PCR was performed using iQ SYBR Green Supermix (Bio-Rad). Relative transcript levels were assessed using the Comparative C_T method. RpL32 was used as an internal control.

SUPPLEMENTAL INFORMATION

Supplemental Information includes Extended Experimental Procedures, six figures, and eight tables and can be found with this article online at http://dx.doi.org/10.1016/j.cell.2013.09.021.

REFERENCES

Alic, N., Hoddinott, M.P., Vinti, G., and Partridge, L. (2011). Lifespan extension by increased expression of the *Drosophila* homologue of the IGFBP7 tumour suppressor. Aging Cell *10*, 137–147.

Andreux, P.A., Houtkooper, R.H., and Auwerx, J. (2013). Pharmacological approaches to restore mitochondrial function. Nat. Rev. Drug Discov. *12*, 465–483.

Bai, J., Hartwig, J.H., and Perrimon, N. (2007). SALS, a WH2-domain-containing protein, promotes sarcomeric actin filament elongation from pointed ends during *Drosophila* muscle growth. Dev. Cell *13*, 828–842.

Berger, I., Elpeleg, O.N., and Saada, A. (1996). Lipoamide dehydrogenase activity in lymphocytes. Clin. Chim. Acta *256*, 197–201.

Boström, P., Wu, J., Jedrychowski, M.P., Korde, A., Ye, L., Lo, J.C., Rasbach, K.A., Boström, E.A., Choi, J.H., Long, J.Z., et al. (2012). A PGC1-α-dependent myokine that drives brown-fat-like development of white fat and thermogenesis. Nature *481*, 463–468.

Clark, I.E., Dodson, M.W., Jiang, C., Cao, J.H., Huh, J.R., Seol, J.H., Yoo, S.J., Hay, B.A., and Guo, M. (2006). *Drosophila* pink1 is required for mitochondrial function and interacts genetically with parkin. Nature *441*, 1162–1166.

Figure 7. ImpL2 Expression Increases Lysosome Biogenesis, Possibly to Augment Autophagic Flux in TDN Muscles
(A) A transgenic UAS-GFP line with a mitochondrial-targeting sequence (mito-GFP) specifically labels mitochondria in flight muscles (Ai) and colocalizes with streptavidin Alexa Fluor 594 staining (Aii) as shown in (Aiii). Scale bar, 20 μm.
(B and C) Representative confocal images from control fly, TD (B) and TDN (Ci–Ciii), flight muscles show UAS-Atg8-GFP expression, a marker of autophagosomes. (Ciii) is a merged image of (Ci) and (Cii). Note the extensive overlap between Atg8-GFP and streptavidin, denoted by the white arrows. Scale bar, 20 μm.
(D–G) Representative TEMs of TD (D) and TDN flight muscles (E–G) show autophagosomes at different stages of formation after 5 days at 27°C. Fully or partially formed autophagosomes are denoted with red or green arrows, respectively. Scale bars, 1 μm.
(H–J) Phalloidin staining is shown in red. The lysosomal marker, Lamp1-GFP (green), is very weakly expressed in TD-white[RNAi] muscles (Hi and Hii) but is robustly expressed in TDN muscles (Ii and Iii) or muscles overexpressing ImpL2 (Ji and Jii). white[RNAi] controls for titration of Gal4; see the Extended Experimental Procedures. Scale bar, 20 μm.
(K) Relative number of lysosomes in *TDN* and *TDN;Def20/+* thoraxes after 5 days at 27°C is shown. The number of lysosomes in *TDN;Def20/+*, assessed as the relative number of punctae that stain for Lamp1-GFP in confocal z stack images, was normalized to the corresponding value for TDN. Error bars denote mean ± SEM. **p < 0.01 (n = 6).
(L) Lifespan curves at 27°C of flies expressing TDN or TD with transgenic RNAi constructs to Atg6, Atg8a, and Atg12 labeled as TDN-Atg6kd, TDN-Atg8akd, or TDN-Atg12kd are presented. Note that the increased lifespan of *TDN* flies outcrossed to white[RNAi] flies (red, TDN-wkd) is abrogated in TDN-Atg6kd, TDN-Atg8akd, or TDN-Atg12kd flies. No lifespan-promoting effects were evident when any of the Atg RNAi lines were crossed to white[RNAi] flies.
(M) Transcript levels in adult TDN-wkd (labeled WT) thoraxes relative to TDN-Atg6kd, TDN-Atg8akd, or TDN-Atg12kd following the induction of RNAi against Atg6, Atg8a, and Atg12, respectively, for 5 days at 27°C are shown. Fold change shown refers to the mean ± SEM (n = 4 independent experiments). *p < 0.05, **p < 0.01, and ***p < 0.001.
See also Table S8.

Copeland, J.M., Cho, J., Lo, T., Jr., Hur, J.H., Bahadorani, S., Arabyan, T., Rabie, J., Soh, J., and Walker, D.W. (2009). Extension of *Drosophila* life span by RNAi of the mitochondrial respiratory chain. Curr. Biol. *19*, 1591–1598.

Dell'agnello, C., Leo, S., Agostino, A., Szabadkai, G., Tiveron, C., Zulian, A., Prelle, A., Roubertoux, P., Rizzuto, R., and Zeviani, M. (2007). Increased longevity and refractoriness to Ca(2+)-dependent neurodegeneration in Surf1 knockout mice. Hum. Mol. Genet. *16*, 431–444.

Demontis, F., and Perrimon, N. (2010). FOXO/4E-BP signaling in *Drosophila* muscles regulates organism-wide proteostasis during aging. Cell *143*, 813–825.

Dillin, A., Hsu, A.L., Arantes-Oliveira, N., Lehrer-Graiwer, J., Hsin, H., Fraser, A.G., Kamath, R.S., Ahringer, J., and Kenyon, C. (2002). Rates of behavior and aging specified by mitochondrial function during development. Science *298*, 2398–2401.

Durieux, J., Wolff, S., and Dillin, A. (2011). The cell-non-autonomous nature of electron transport chain-mediated longevity. Cell *144*, 79–91.

Evdokimova, V., Tognon, C.E., Benatar, T., Yang, W., Krutikov, K., Pollak, M., Sorensen, P.H., and Seth, A. (2012). IGFBP7 binds to the IGF-1 receptor and blocks its activation by insulin-like growth factors. Sci. Signal. *5*, ra92.

Finley, L.W., and Haigis, M.C. (2009). The coordination of nuclear and mitochondrial communication during aging and calorie restriction. Ageing Res. Rev. *8*, 173–188.

Glembotski, C.C. (2011). Functions for the cardiomyokine, MANF, in cardioprotection, hypertrophy and heart failure. J. Mol. Cell. Cardiol. *51*, 512–517.

Greene, J.C., Whitworth, A.J., Kuo, I., Andrews, L.A., Feany, M.B., and Pallanck, L.J. (2003). Mitochondrial pathology and apoptotic muscle degeneration in *Drosophila* parkin mutants. Proc. Natl. Acad. Sci. USA *100*, 4078–4083.

Hamanaka, R.B., and Chandel, N.S. (2010). Mitochondrial reactive oxygen species regulate cellular signaling and dictate biological outcomes. Trends Biochem. Sci. *35*, 505–513.

Hamilton, B., Dong, Y., Shindo, M., Liu, W., Odell, I., Ruvkun, G., and Lee, S.S. (2005). A systematic RNAi screen for longevity genes in *C. elegans*. Genes Dev. *19*, 1544–1555.

Haynes, C.M., and Ron, D. (2010). The mitochondrial UPR - protecting organelle protein homeostasis. J. Cell Sci. *123*, 3849–3855.

Hollinshead, M., Sanderson, J., and Vaux, D.J. (1997). Anti-biotin antibodies offer superior organelle-specific labeling of mitochondria over avidin or streptavidin. J. Histochem. Cytochem. *45*, 1053–1057.

Honegger, B., Galic, M., Köhler, K., Wittwer, F., Brogiolo, W., Hafen, E., and Stocker, H. (2008). Imp-L2, a putative homolog of vertebrate IGF-binding protein 7, counteracts insulin signaling in *Drosophila* and is essential for starvation resistance. J. Biol. *7*, 10.

Karpac, J., Younger, A., and Jasper, H. (2011). Dynamic coordination of innate immune signaling and insulin signaling regulates systemic responses to localized DNA damage. Dev. Cell *20*, 841–854.

Kirchman, P.A., Kim, S., Lai, C.Y., and Jazwinski, S.M. (1999). Interorganelle signaling is a determinant of longevity in Saccharomyces cerevisiae. Genetics *152*, 179–190.

Kutsukake, M., Ishihara, R., Momose, K., Isaka, K., Itokazu, O., Higuma, C., Matsutani, T., Matsuda, A., Sasajima, K., Hara, T., and Tamura, K. (2008). Circulating IGF-binding protein 7 (IGFBP7) levels are elevated in patients with endometriosis or undergoing diabetic hemodialysis. Reprod. Biol. Endocrinol. *6*, 54.

Liu, Z., and Butow, R.A. (2006). Mitochondrial retrograde signaling. Annu. Rev. Genet. *40*, 159–185.

Liu, X., Jiang, N., Hughes, B., Bigras, E., Shoubridge, E., and Hekimi, S. (2005). Evolutionary conservation of the clk-1-dependent mechanism of longevity: loss of mclk1 increases cellular fitness and lifespan in mice. Genes Dev. *19*, 2424–2434.

Lubos, E., Loscalzo, J., and Handy, D.E. (2011). Glutathione peroxidase-1 in health and disease: from molecular mechanisms to therapeutic opportunities. Antioxid. Redox Signal. *15*, 1957–1997.

McGuire, S.E., Mao, Z., and Davis, R.L. (2004). Spatiotemporal gene expression targeting with the TARGET and gene-switch systems in *Drosophila*. Sci. STKE *2004*, pl6.

Migliaccio, E., Giorgio, M., Mele, S., Pelicci, G., Reboldi, P., Pandolfi, P.P., Lanfrancone, L., and Pelicci, P.G. (1999). The p66shc adaptor protein controls oxidative stress response and life span in mammals. Nature *402*, 309–313.

Missirlis, F., Rahlfs, S., Dimopoulos, N., Bauer, H., Becker, K., Hilliker, A., Phillips, J.P., and Jäckle, H. (2003). A putative glutathione peroxidase of *Drosophila* encodes a thioredoxin peroxidase that provides resistance against oxidative stress but fails to complement a lack of catalase activity. Biol. Chem. *384*, 463–472.

Orsini, F., Migliaccio, E., Moroni, M., Contursi, C., Raker, V.A., Piccini, D., Martin-Padura, I., Pelliccia, G., Trinei, M., Bono, M., et al. (2004). The life span determinant p66Shc localizes to mitochondria where it associates with mitochondrial heat shock protein 70 and regulates trans-membrane potential. J. Biol. Chem. *279*, 25689–25695.

Owusu-Ansah, E., and Banerjee, U. (2009). Reactive oxygen species prime *Drosophila* haematopoietic progenitors for differentiation. Nature *461*, 537–541.

Owusu-Ansah, E., Yavari, A., Mandal, S., and Banerjee, U. (2008). Distinct mitochondrial retrograde signals control the G1-S cell cycle checkpoint. Nat. Genet. *40*, 356–361.

Peternelj, T.T., and Coombes, J.S. (2011). Antioxidant supplementation during exercise training: beneficial or detrimental? Sports Med. *41*, 1043–1069.

Powers, S.K., Duarte, J., Kavazis, A.N., and Talbert, E.E. (2010). Reactive oxygen species are signalling molecules for skeletal muscle adaptation. Exp. Physiol. *95*, 1–9.

Raimundo, N., Song, L., Shutt, T.E., McKay, S.E., Cotney, J., Guan, M.X., Gilliland, T.C., Hohuan, D., Santos-Sacchi, J., and Shadel, G.S. (2012). Mitochondrial stress engages E2F1 apoptotic signaling to cause deafness. Cell *148*, 716–726.

Rera, M., Bahadorani, S., Cho, J., Koehler, C.L., Ulgherait, M., Hur, J.H., Ansari, W.S., Lo, T., Jr., Jones, D.L., and Walker, D.W. (2011). Modulation of longevity and tissue homeostasis by the *Drosophila* PGC-1 homolog. Cell Metab. *14*, 623–634.

Ristow, M., and Zarse, K. (2010). How increased oxidative stress promotes longevity and metabolic health: the concept of mitochondrial hormesis (mitohormesis). Exp. Gerontol. *45*, 410–418.

Rubinsztein, D.C., Codogno, P., and Levine, B. (2012). Autophagy modulation as a potential therapeutic target for diverse diseases. Nat. Rev. Drug Discov. *11*, 709–730.

Rusten, T.E., Lindmo, K., Juhász, G., Sass, M., Seglen, P.O., Brech, A., and Stenmark, H. (2004). Programmed autophagy in the *Drosophila* fat body is induced by ecdysone through regulation of the PI3K pathway. Dev. Cell *7*, 179–192.

Schulz, T.J., Zarse, K., Voigt, A., Urban, N., Birringer, M., and Ristow, M. (2007). Glucose restriction extends *Caenorhabditis elegans* life span by inducing mitochondrial respiration and increasing oxidative stress. Cell Metab. *6*, 280–293.

Teleman, A.A., Chen, Y.W., and Cohen, S.M. (2005). 4E-BP functions as a metabolic brake used under stress conditions but not during normal growth. Genes Dev. *19*, 1844–1848.